
EURO-COST

SOURCE: ¹Technische Universität Wien, Institut für
Nachrichtentechnik und Hochfrequenz-
technik, Wien, Österreich
 ²Aalborg University, Departement of Com-
munication Technology, Aalborg, Denmark

**Cluster Angular Spread Estimation
for MIMO Indoor Environments**

Nicolai Czink¹, Xuefeng Yin²
Gußhausstraße 25/389 1040 Wien AUSTRIA
Phone: +43 (1) 58801 38979
Fax: +43 (1) 58801 38999
Email: nicolai.czink@tuwien.ac.at

Cluster Angular Spread Estimation for MIMO indoor environments

Nicolai Czink¹

nicolai.czink@tuwien.ac.at
Institut für Nachrichtentechnik
und Hochfrequenztechnik
Technische Universität Wien
Gusshausstraße 25/389,
A-1040 Wien, Austria

Xuefeng Yin²

xuefeng.yin@kom.auc.dk
Department of Communication Technology
Institute of Electronic Systems
Aalborg University
Niels Jernes Vej 12,
DK-9220 Aalborg, Denmark

Abstract

An important parameter of MIMO channel models is the cluster root-mean-square (rms) directional spread. We introduce a novel method to estimate cluster rms spreads from measurements. We use the SAGE algorithm to extract propagation paths, from which we define clusters in the angular domain, and subsequently estimate the cluster spreads based solely on propagation paths within the clusters. To check the accuracy, we applied our estimator on synthetic scenarios with known angular spread values. We find that the estimator is approximately unbiased, and provides consistent estimates with insignificant errors.

1 Introduction

The use of multiple antennas at both link ends (MIMO) in wireless communications promises high spectral efficiency and reliability. Accurate channel models are required for proper design of signal processing algorithms. An important feature of the MIMO propagation channel with respect to MIMO applications is the occurrence of multi-path components (MPCs) in clusters. The authors of [1] have shown that channel models disregarding clustering effects overestimate channel capacity. Several new models assume clustered propagation paths, where propagation paths within a cluster show a distinct “angular spread” [2, 3]. In this paper we use the measure of the “directional spread” as it is a more accurate description of the spread of the MPCs. Please refer to [4] for detailed discussion of the different meanings and implications.

This paper introduces and validates a novel estimator to extract the clusters’ directional spreads from measurements in multiple-cluster environments. The method is a three-step procedure: (i) Estimate propagation paths using the SAGE algorithm, (ii) identify clusters visually, (iii) use only propagation paths within a cluster to estimate the cluster’s directional spread.

Though we have encouraging data from measurements available, we prefer to check the performance of the estimator with synthetic scenarios. Accuracy and (non)-biasedness can only be assessed by these means.

2 Method

2.1 System Model

For the calculations we use an 8×8 flat-fading MIMO system, using uniform linear arrays (ULA) at both link ends, however our method can easily be extended to arbitrary array configurations and sizes. The cluster spreads and positions are assumed to be constant over time,

hence the channel is wide-sense stationary. So we can consider multiple channel realisations of the scenario. For further evaluations we use a number of 150 realisations.

2.2 Synthetic Scenarios

To check the accuracy of the estimators to be introduced for the directional spreads, we created synthetic scenarios and performed our estimation algorithms on them.

For the synthetic scenarios, we generated channel matrices for an 8×8 MIMO system, where the receiver and the transmitter are equipped with ULAs consisting of 8 isotropic antennas spaced by half a wavelength.

For each scenario, a number of N_c clusters were simulated in the synthetic environment, where N_c is an integer randomly selected between 2 and 6. The centre positions of the clusters are independently, uniformly selected in $[-60^\circ, +60^\circ]$ for azimuth of arrival (AoA) and $[-90^\circ, +90^\circ]$ for azimuth of departure (AoD). To avoid heavily overlapped clusters, the centres of any two clusters are spaced at least 20° in AoA.

For each realisation we assigned MPCs to the clusters. Each individual cluster consists of L MPCs, where L is an integer randomly selected between 10 and 100. The AoAs and AoDs of the MPCs in each cluster are independent truncated Gaussian distributed random variables¹ with directional spread $\theta_{\text{AoA}/\text{AoD}}^{\text{rms}}$. The AoA and AoD directional spreads of the MPCs are randomly selected from the set $\theta_{\text{AoA}/\text{AoD}}^{\text{rms}} \in \{0.1^\circ, 1^\circ, 2^\circ, \dots, 8^\circ\}$ to assess the performance of the estimator at distinctive cluster sizes.

Two fading scenarios, i.e. Rayleigh and Rice fading, are considered in the simulations. For Rayleigh fading, the MPCs are characterized with equal amplitude and independent $[0, 2\pi)$ -uniformly-distributed random phases. The phases are uncorrelated with the AoAs and the AoDs of the MPCs. In the scenario of Rice fading, the MPCs, except for the MPC located at the centre of the cluster, have equal amplitudes and $[0, 2\pi)$ -uniformly-distributed random phases. The component located at the centre of the cluster has an amplitude larger than the other MPCs and a deterministic phase, which is randomly selected initially. The Rice factor is the ratio between the power of this central wave and that of the other components. Notice that in the simulation, we specify Rice fading for the clusters with the directional spread of 0.1° , and randomly choose between Rice and Rayleigh fading scenarios for the clusters with the directional spread larger than or equal to 1° . This consideration is based on physical wave propagation, as clusters showing very small directional spread can be considered as point sources or specular reflections, which have to show deterministic behaviour. Thus, such clusters exhibit Rician fading. When the directional spread is large, both Rice or Rayleigh fading scenarios are possible.

The signal-to-noise ratio (SNR) was defined as the ratio between the mean power of the received signals contributed by the clusters and the variance of the noise at each Rx antenna, and was set to 50dB.

2.3 Estimation of cluster directional spread

The estimation of the cluster directional spread was done in three steps: SAGE estimation, cluster identification and cluster spread estimation.

¹We use truncated Gaussian distribution as an approximation of von-Mises distribution for clusters with small directional spreads. According to [4], the von-Mises PDF is proposed to describe the azimuth distribution of the MPCs in a cluster. The truncated Gaussian PDFs are considered to be identical with the von-Mises PDF when the parameter κ of the von-Mises PDF is larger than 16, or equivalently when the directional spread $\theta^{\text{rms}} < 14.3^\circ$. In this case κ can be approximated by $\kappa \approx 1/(\theta^{\text{rms}})^2$.

2.3.1 SAGE estimation

We used the SAGE algorithm [5] (implementation from [6]) on each of our channel realisations individually to estimate the complex amplitudes, AoAs, and AoDs of the propagation paths. SAGE estimation has to be performed conscientiously. For the model order we chose the maximum value of 49, to extract as many paths as possible for 8×8 MIMO systems. The dynamic range was set to 30dB to be well within the SNR level of our synthetic channels. With these settings we made sure not to extract more information from the channel matrices as there is inherently provided.

2.3.2 Cluster identification

Throughout literature (e.g. [2, 7]), clusters are identified visually, as clustering algorithms are either too time consuming, or do not work properly. We also adopted this approach, but improve it by using the double-directional angular power spectrum (APS) jointly with SAGE estimates of the channel parameters.

Once clusters have been identified, the directional distributions can be determined. One has to be careful with the estimation of the cluster directional spread. Evolving from the propagation model used, directional distributions are not correctly reproduced by high-resolution estimation algorithms that base on the specular path model [8]. We circumvented this effect by *limiting our clusters by ellipses*.

For each scenario, we considered $K = 150$ different realisations of the 8×8 MIMO channel matrix \mathbf{H}_k , where k denotes the k th realisation.

For visual cluster identification, we used the following method. Channel matrices were averaged by using the full spatial correlation matrix, \mathbf{R}_H , which was estimated by

$$\mathbf{R}_H = \frac{1}{K} \sum_{i=1}^K \text{vec}(\mathbf{H}_i) \text{vec}(\mathbf{H}_i)^H, \quad (1)$$

where $(\cdot)^H$ denotes hermitian transpose, and the $\text{vec}(\cdot)$ operator stacks the columns of a matrix into a vector. By this, we average over small-scale and frequency selective fading effects.

The double-directional angular power spectrum (APS) [9] was calculated using the Bartlett beamformer [10] by

$$P(\varphi_{R_x}, \varphi_{T_x}) = (\mathbf{a}_{T_x}(\varphi_{T_x}) \otimes \mathbf{a}_{R_x}(\varphi_{R_x}))^H \mathbf{R}_H ((\mathbf{a}_{T_x}(\varphi_{T_x}) \otimes \mathbf{a}_{R_x}(\varphi_{R_x}))), \quad (2)$$

where \otimes denotes the Kronecker product, $\mathbf{a}_{R_x}(\varphi_{R_x})$ the normalised response vector from AoA, φ_{R_x} , and $\mathbf{a}_{T_x}(\varphi_{T_x})$ the normalised steering vector for AoD, φ_{T_x} .

To find multipath clusters, we plotted two figures: (i) the APS from (2), jointly with the 1000 strongest SAGE estimation points, and (ii) these SAGE estimates only, but colour-coded, indicating their power. Then we defined clusters in the APS by matching the SAGE estimates to the APS. Clusters show dense SAGE estimates with similar powers. Hence, clusters were defined by assigning ellipses in the APS, fitting both, the APS and the SAGE estimates, best.

2.3.3 Cluster allocation

Characteristics of the defined clusters were gathered by using the SAGE estimates allocated to clusters. The allocation was done for each scenario by the following algorithm.

1. SAGE estimation provides an indexed set of complex amplitudes, \underline{A}_k , AoAs, $\underline{\varphi}_{\text{Rx},k}$ and AoDs, $\underline{\varphi}_{\text{Tx},k}$ of the propagation paths, for each considered channel realisation k . The set \underline{A}_k is indexed by

$$\underline{A}_k = \left(A_k^{(1)} \quad A_k^{(2)} \quad \dots \quad A_k^{(N_{\text{p},k})} \right), \quad (3)$$

where each of the sets contain $N_{\text{p},k}$ (the number of resolved paths in the k th channel realisation) elements, at most 49 (corresponding to the model order). Equal indexing is done for $\underline{\varphi}_{\text{Rx},k}$ and $\underline{\varphi}_{\text{Tx},k}$.

Those sets are collected in Θ_k given by

$$\Theta_k = \left(\underline{A}_k \quad \underline{\varphi}_{\text{Rx},k} \quad \underline{\varphi}_{\text{Tx},k} \right) = \text{SAGE}(\mathbf{H}_k), \quad (4)$$

describing all resolved (estimated) paths for the k th channel realisation, where $\text{SAGE}(\cdot)$ represents the estimates returned by the SAGE algorithm.

2. For each cluster l , we allocated the SAGE estimates enclosed by the defined ellipse and collected them in cluster sets \mathcal{C}_l by

$$\mathcal{C}_l = \left(\tilde{\Theta}_{1l} \quad \tilde{\Theta}_{2l} \quad \dots \quad \tilde{\Theta}_{Kl} \right), \quad l = 1 \dots N_c, \quad (5)$$

where N_c denotes the number of clusters in the considered scenario and $\tilde{\Theta}_{kl}$ is a subset of Θ_k containing the corresponding SAGE estimates for the considered cluster l and channel realisation k ,

$$\tilde{\Theta}_{kl} = \left(\tilde{\underline{A}}_{kl} \quad \tilde{\underline{\varphi}}_{\text{Rx},kl} \quad \tilde{\underline{\varphi}}_{\text{Tx},kl} \right), \quad \tilde{\Theta}_{kl} \subset \Theta_k.$$

The indexed subsets $\tilde{\underline{A}}_{kl}$, $\tilde{\underline{\varphi}}_{\text{Rx},kl}$ and $\tilde{\underline{\varphi}}_{\text{Tx},kl}$ hold $N_{\text{p},kl}$ (number of allocated paths in the k th realisation for the l th cluster) elements, each, and are again indexed as shown in (3). The sorting of the SAGE estimates into the cluster sets was done by geometrical considerations in the angular domain.

Figure 1 shows the double-directional APS of the exemplary synthetic scenario. Identified clusters are enclosed by ellipses; SAGE estimates falling within these ellipses are shown as white crosses. The other estimates are discarded.

2.3.4 Cluster directional spread

In this paper, we evaluate the root-mean-square (rms) *cluster* directional spread. This approach extends the view of a global directional spread of the environment.

Due to our method using SAGE estimates based on the specular wave model, we only state a value of the cluster rms directional spread, and not a distribution function of the cluster spread, as this would yield demonstrably false results [8].

The *global* directional spread of a propagation environment [4] is correctly defined by the second order moment of the *directions* at the Rx and Tx, where the direction is described by the spherical unity vector Ω , hence²

²In a cartesian coordinate system, Ω is a vector given by $\Omega \doteq [\cos(\varphi) \sin(\vartheta), \sin(\varphi) \sin(\vartheta), \cos(\vartheta)]^T$, where φ and ϑ denote azimuth and elevation, respectively.

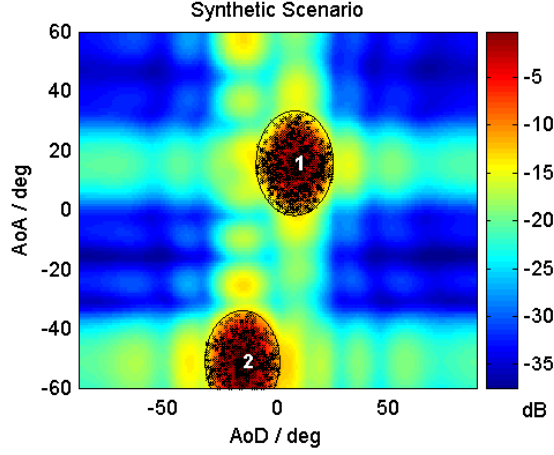


Figure 1: Double-directional APS with identified clusters (ellipses) and allocated SAGE estimates (crosses) of synthetic indoor scenario

$$\Omega^{\text{rms}} = \sqrt{\frac{\int_{-\pi}^{\pi} |\Omega - \bar{\Omega}|^2 |A(\Omega)|^2 d\Omega}{\int_{-\pi}^{\pi} |A(\Omega)|^2 d\Omega}} \quad (6)$$

with

$$\bar{\Omega} = \frac{\int_{-\pi}^{\pi} \Omega |A(\Omega)|^2 d\Omega}{\int_{-\pi}^{\pi} |A(\Omega)|^2 d\Omega}, \quad (7)$$

where Ω^{rms} denotes the directional spread and $|A(\Omega)|^2$ the directional power spectrum.

Multipath clusters in indoor scenarios show very low directional spreads. Hence, to derive the cluster spread, we take the freedom to use the following approximation for *small* global directional spread values in horizontal propagation [11], which is given by

$$\theta^{\text{rms}} = \sqrt{\frac{\int_{-\pi}^{\pi} (\theta - \bar{\theta})^2 |A(\theta)|^2 d\theta}{\int_{-\pi}^{\pi} |A(\theta)|^2 d\theta}}, \quad \text{with } \bar{\theta} = \frac{\int_{-\pi}^{\pi} \theta |A(\theta)|^2 d\theta}{\int_{-\pi}^{\pi} |A(\theta)|^2 d\theta}, \quad (8)$$

where θ denotes the angle, and $|A(\theta)|^2$ the angular power spectrum. In these formulas, integration over the whole angular domain is performed³.

In the case of the *cluster* directional spread [12], only those components that contribute to the considered cluster have to be accounted. As our propagation paths are assumed to be discrete, the integrals reduce to sums and can easily be evaluated.

For estimation of the cluster directional spreads, we calculated the AoA and AoD rms directional spread for each cluster l , by using the powers and angles of all resolved paths in the cluster. The mean AoA and AoD were separately calculated by

$$\bar{\theta}_{\text{AoA/AoD},l} = \frac{\sum_{k=1}^K \sum_{n=1}^{N_{p,k}} \tilde{\varphi}_{\text{Rx/Tx},kl}^{(n)} |\tilde{A}_{kl}^{(n)}|^2}{\sum_{k=1}^K \sum_{n=1}^{N_{p,k}} |\tilde{A}_{kl}^{(n)}|^2}, \quad (9)$$

³We want to note that this definition is sometimes used for the global directional spread, even when multiple large clusters are observed, which is not sensible.

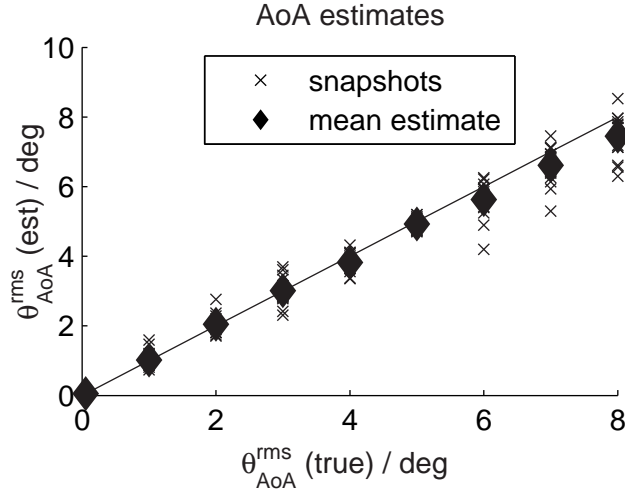


Figure 2: Directional spread estimation results for synthetic scenarios with distinct cluster spreads. Crosses indicate estimates from the different clusters, diamonds indicate the mean estimates. The estimator is approximately unbiased.

subsequently, the rms directional spread was obtained by

$$\hat{\theta}_{\text{AoA}/\text{AoD},l}^{\text{rms}} = \sqrt{\frac{\sum_{k=1}^K \sum_{n=1}^{N_{p,k}} (\hat{\varphi}_{\text{Rx}/\text{Tx},kl}^{(n)} - \bar{\theta}_{\text{AoA}/\text{AoD},l})^2 |\tilde{A}_{kl}^{(n)}|^2}{\sum_{k=1}^K \sum_{n=1}^{N_{p,k}} |\tilde{A}_{kl}^{(n)}|^2}}, \quad (10)$$

for each cluster l in the AoA (Rx) and AoD (Tx) domain.

2.4 Accuracy of estimators

The previously introduced estimators are used on the synthetic scenarios. We will present results for estimation of the AoA directional spreads $\hat{\theta}_{\text{AoA}}^{\text{rms}}$ only, as the estimator shows similar results for the AoD directional spreads $\hat{\theta}_{\text{AoD}}^{\text{rms}}$. Figure 2 demonstrates the estimator performance for different cluster spreads. The estimates for each cluster are shown as crosses, the mean estimate for a distinct AoA is denoted as solid diamond. The mean values of the estimates correspond to the true spreads very well, hence, the estimator is approximately unbiased in the considered range.

The accuracy of the estimator can be seen in Figure 3, where the absolute errors, relative to the true value are plotted (crosses) together with their mean values (circles) and rms values (diamonds) for each distinct AoA. These errors are approximately 10% on average for the directional spread $\theta_{\text{AoA}}^{\text{rms}} > 1^\circ$, and equal 40% for the directional spread close to 0° . This shows that the performance of the directional spread estimator is sensitive to small spreads. However, when the true directional spread is small, the absolute error is insignificant, e.g. it is approximately 0.04° in average for $\theta_{\text{AoA}}^{\text{rms}} = 0.1^\circ$. Thus from a practical point of view the estimates obtained with small directional spreads are acceptable. We concluded from the above observations that the proposed algorithm provides consistent estimates in the directional spread estimation with insignificant errors.

3 Conclusions

We introduced a novel estimator to extract rms directional cluster spreads from measurements in MIMO indoor environments. The method bases on three steps: SAGE estimation of propa-

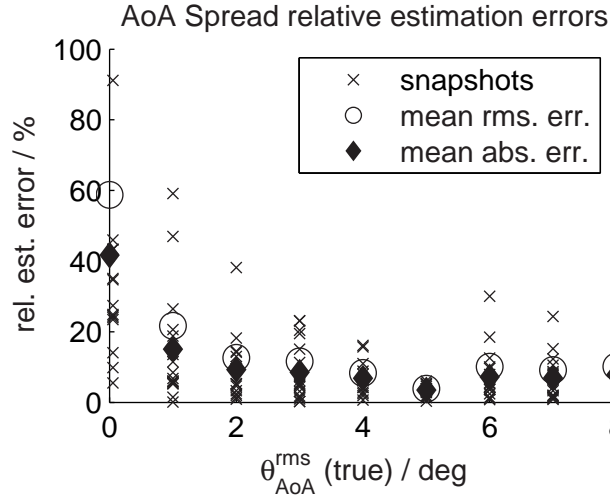


Figure 3: Errors of directional spread estimation for synthetic scenarios. The absolute errors relative to the true errors are evaluated for distinct cluster spreads. Crosses indicate estimates from the different clusters, circles the mean errors and diamonds the rms errors for the different cluster spreads.

gation paths, identification of clusters, and estimating the cluster spreads.

Identification of clusters was done visually using the double-directional APS jointly with SAGE estimates. Ellipses were defined to fit the clusters best. The cluster directional spread was estimated by using only propagation paths within the considered cluster.

We assessed the accuracy and (non)-biasedness of the estimator using synthetic scenarios with known spread values and found that the estimator is largely unbiased in the considered range and shows only insignificant estimation errors.

Acknowledgements

Part of this work was supported by the European-Commission-funded Network of Excellence NEWCOM.

References

- [1] K. Li, M. Ingram, and A. Van Nguyen, "Impact of clustering in statistical indoor propagation models on link capacity," *IEEE Transactions on Communications*, vol. 50, no. 4, pp. 521 – 523, April 2002.
- [2] C.-C. Chong, C.-M. Tan, D. Laurenson, S. McLaughlin, M. Beach, and A. Nix, "A new statistical wideband spatio-temporal channel model for 5-GHz band WLAN systems," *IEEE Journal on Selected Areas in Communications*, vol. 21, no. 2, pp. 139 – 150, Feb. 2003.
- [3] Q. H. Spencer, B. D. Jeffs, M. A. Jensen, and A. L. Swindlehurst, "Modeling the statistical time and angle of arrival characteristics of an indoor multipath channel," *IEEE Journal on Selected Areas in Communications*, vol. 18, pp. 347 – 359, March 2000.
- [4] B. H. Fleury, "First- and second-order characterization of direction dispersion and space selectivity in the radio channel," *IEEE Transactions on Information Theory*, vol. IT-46, no. 6, pp. 2027–2044, September 2000.

- [5] B. H. Fleury, M. Tschuddin, R. Heddergott, D. Dahlhaus, and K. I. Pedersen, "Channel parameter estimation in mobile radio environments using the SAGE algorithm," no. 3, pp. 434–450, 18 1999.
- [6] S. Semmelrodt, R. Kattenbach, and H. Früchtling, "Toolbox for spectral analysis and linear prediction of stationary and non-stationary signals," *COST 273 TD(04)019*, Athens, Greece, January 26–28, 2004.
- [7] K. Yu, Q. Li, D. Cheung, and C. Prettie, "On the tap and cluster angular spreads of indoor WLAN channels," in *Proceedings of IEEE Vehicular Technology Conference Spring 2004*, Milano, Italy, May 17–19, 2004.
- [8] M. Bengtsson and B. Volcker, "On the estimation of azimuth distributions and azimuth spectra," *IEEE Vehicular Technology Conference*, vol. 3, no. 54, pp. 1612 – 1615, October 07–11, 2001, Atlantic City, NJ, USA.
- [9] M. Steinbauer, A. Molisch, and E. Bonek, "The double-directional radio channel," *IEEE Antennas and Propagation Magazine*, vol. 43, no. 4, pp. 51 – 63, Aug. 2001.
- [10] M. Bartlett, "Smoothing periodograms from time series with continuous spectra," *Nature*, vol. No. 161, 1948.
- [11] P. Eggers, "Angular propagation descriptions relevant for base station adaptive antenna operations," *Kluwer Wireless Personal Communications, Special Issue on SDMA*, vol. 11, pp. 3–29, 1999.
- [12] A. Kuchar, M. Tangemann, and E. Bonek, "A real-time DOA-based smart antenna processor," *IEEE Transactions on Vehicular Technology*, vol. 51, no. 6, pp. 1279–1293, November 2002.